Immunity
Article

# Human and Mouse Granzyme A Induce a Proinflammatory Cytokine Response

Sunil S. Metkar,[1] Cheikh Menaa,[1] Julian Pardo,[2,3] Baikun Wang,[1] Reinhard Wallich,[4] Marina Freudenberg,[3] Stephen Kim,[1] Srikumar M. Raja,[1] Lianfa Shi,[1] Markus M. Simon,[3] and Christopher J. Froelich[1,*]
[1]Department of Medicine, NorthShore University HealthSystem Research Institute, Evanston, IL 60201, USA
[2]Department of Biochemistry and Molecular and Cellular Biology; Faculty of Science, University of Zaragoza, 50009 Zaragoza, Spain
[3]Metschnikoff Laboratory, Max-Planck-Institut für Immunbiologie, 79108 Freiburg, Germany
[4]Institute for Immunology, University of Heidelberg, 69120 Heidelberg, Germany
*Correspondence: c-froelich@northwestern.edu
DOI 10.1016/j.immuni.2008.08.014

## SUMMARY

**Granzyme A (GzmA) is considered a major proapoptotic protease. We have discovered that GzmA-induced cell death involves rapid membrane damage that depends on the synergy between micromolar concentrations of GzmA and sublytic perforin (PFN). Ironically, GzmA and GzmB, independent of their catalytic activity, both mediated this swift necrosis. Even without PFN, lower concentrations of human GzmA stimulated monocytic cells to secrete proinflammatory cytokines (interleukin-1β [IL-1β], TNFα, and IL-6) that were blocked by a caspase-1 inhibitor. Moreover, murine GzmA and GzmA$^+$ cytotoxic T lymphocytes (CTLs) induce IL-1β from primary mouse macrophages, and *GzmA*$^{-/-}$ mice resist lipopolysaccharide-induced toxicity. Thus, the granule secretory pathway plays an unexpected role in inflammation, with GzmA acting as an endogenous modulator.**

## INTRODUCTION

Cytotoxic cells employ two distinct strategies to eliminate targeted cells: engagement of death receptors and the granule secretory pathway. Cytotoxic cell granule-mediated cell death involves perforin (PFN) and a family of granule-associated serine proteases, termed granzymes (Gzms). Originally described in the mid 1980s (Masson and Tschopp, 1987), Gzms have been postulated to play a number of biological roles; they have been thought to act as death effectors or be involved in extracellular matrix degradation or viral inactivation (Kramer and Simon, 1987; Masson and Tschopp, 1987).

The first description of mouse native GzmA (nMuGzmA) as being a cytotoxic serine protease was published by the Henkart lab, which showed that treatment of EL-4 target cells with isolated native nMuGzmA and mouse PFN (nMuPFN) caused substantial target DNA breakdown (Hayes et al., 1989). Shortly thereafter, Greenberg and Shi isolated native rat GzmA (nRatGzmA), observing that the protease could induce apoptosis (DNA fragmentation) in the presence of rat PFN (Shi et al., 1992). At the same time, Shiver et al. reported that transfection of rat basophilic leukemia (RBL) cells with both MuGzmA and MuPFN genes endowed the line with the potential to induce target cell DNA breakdown (Shiver et al., 1992).

Subsequently, *GzmB*$^{-/-}$ mice, which lack GzmB but express GzmA and PFN, were generated, and the evaluation of antitumor host defense clearly established that GzmB is critical for granule-mediated apoptosis in vitro (Heusel et al., 1994). In comparison, the phenotype of *GzmA*$^{-/-}$ mice was unexpectedly nondescript, showing that antitumor host defense was not diminished, but deficits against ectromelia mouse pox virus were noted (Ebnet et al., 1995; Mullbacher et al., 1996). As a means of reconciling the apparent inconsistencies, the results for GzmA were attributed to functional redundancy of the granule proteases.

For verification of the cytotoxic effect of GzmA, recombinant human GzmA (rHuGzmA) was produced and shown to mediate, together with rat PFN, a form of cell death that was associated with prominent membrane damage (Beresford et al., 1999a). Subsequent studies showed that rHuGzmA, when delivered with rat PFN, cleaves a number of intracellular substrates, with the most crucial being disruption of DNA-repair programs (SET and APE-1) (Beresford et al., 2001; Fan et al., 2003a; Fan et al., 2003b; Martinvalet et al., 2005; Zhang et al., 2001). Furthermore, ex vivo cytotoxic T lymphocytes (CTLs) of GzmB$^{(-/-)}$ mice were found to induce apoptosis by multiple criteria (Pardo et al., 2004). Taken together, the data strongly supported the original concept that GzmA was indeed lethal.

Using nHuGzmA, without contaminating nHuGzmB, and rHuGzmA, we show here in both short-term cell-death assays and a long-term proliferative assay that the proteases lack cytotoxic activity after intracellular delivery with either HuPFN or Adenoviral particles. Furthermore, evidence indicates that nMuGzmA and rMuGzmA also fail to induce target cell death after intracellular delivery. GzmA was only cytotoxic when micromolar concentrations were combined with rat PFN, and then the cells succumbed to necrosis due to virtually instantaneous membranolysis.

Considering alternate biological functions, we find that nHuGzmA and rHuGzmA (but not inactive protease) induce human adherent peripheral blood mononuclear cells (PBMCs) to express a proinflammatory cytokine profile consisting of interleukin-1β (IL-1β), IL-6, IL-8, and TNF-α. Signaling by HuGzmA appears to require internalization of the protease rather than engagement of transmembrane receptors, and the resultant cytokine expression occurs in the presence of caspase-1 activation. Taken together, the data suggest that human and murine GzmA do not directly contribute to cell death. Instead, the

tryptase appears to initiate a proinflammatory cytokine cascade that may involve components of the recently described cytosolic pattern-recognition system (Franchi et al., 2006). To our knowledge, GzmA may represent the first description of an endogenous mediator that engages this system to induce expression of IL-1β, providing an important link between cytotoxic cells and the innate immune response.

## RESULTS

### Characterization of Native Human Granzyme A

nHuGzmA was isolated from cytotoxic granules of the NK92 lymphoma cell line with accepted methodology (Hanna et al., 1993). Immunoblot with GzmA, GzmB, and GzmM antibodies (Abs) showed that nHuGzmA was not contaminated with GzmB or GzmM (Figure 1A). The esterolytic activity of nHuGzmA and rHuGzmA (Axxora) were comparable (Figure 1B) (specific activity was ~120 U/μg for nHuGzmA and ~110 U/μg for rHuGzmA). Finally, the dimeric status of the nHuGzmA was confirmed by SDS-PAGE and immunoblotting (Figures 1C and 1D).

To ensure that target cells internalized active nHuGzmA, we then evaluated the binding and internalization of the labeled protease. Jurkat cells were treated with increasing concentrations of $nHuGzmA_{488}$ for 30 min on ice (binding) (Raja et al., 2005) or at 37°C (internalization). As reported for nHuGzmB (Raja et al., 2005), the Ka of the dimeric nHuGzmA for Jurkat cells was approximately 1.0 nM (Figure 1E). $nHuGzmA_{488}$ was internalized at all concentrations exceeding the putative Ka (Figure 1F). Internalization was confirmed by confocal microscopy in which an endosomal pattern was noted (Figure 1G). To investigate clearance of nHuGzmA from the cell surface, we conducted a pulse-wash analysis that showed that more than 70% of the granzyme was internalized within 5 min (Figure 1H).

### nHuGzmA Lacks Cytotoxic Activity with Human PFN and Adenoviral Particles

Having confirmed that Jurkat cells bind and internalize nHuGzmA, we examined the cytotoxic potency of the protease against this cell line as well as other cell lines that are reportedly sensitive to the effects of the tryptase (Beresford et al., 1999a). The intracellular delivery of nHuGzmA and nHuGzmB was performed with both HuPFN and Adenoviral particles (AD), with the latter included for elimination of potentially uncontrollable effects of PFN (Froelich et al., 2004). After 90 min incubation, mitochondrial-membrane depolarization, plasma-membrane permeability, and reactive oxygen species (ROS) generation were measured. AD effectively delivered nHuGzmB, causing efficient mitochondrial-potential loss, ROS generation, and membrane damage. The intracellular delivery of nHuGzmA by AD, however, was not associated with alteration in these variables (Figure 2A). Measurement of these parameters after shorter incubation times (5 min to 60 min) also yielded similar results (data not shown). When HeLa cells were used as targets, only AD-mediated delivery of GzmB caused disruption of mitochondrial-membrane potential or damage to the plasma membrane (Figure 2B).

Although nHuGzmA appeared to lack cytotoxic activity if applied to target cells in the presence of AD, it was possible that PFN might synergize with the tryptase to kill target cells. The toxicity of nHuGzmA and rHuGzmA was tested with a cell line (U937) reportedly susceptible to rHuGzmA in the presence of rat PFN (Beresford et al., 1999a). For ensuring that an effective concentration of HuPFN was used to deliver the proteases, nHuGzmB (1 μg/ml [30 nM]) acted as the positive control. In comparison to nHuGzmB, nHuGzmA and rHuGzmA were added to the targets at a 10-fold higher concentration (10 μg/ml; 192 nM for dimer). Despite the 10-fold higher concentrations, neither form of HuGzmA altered the mitochondrial-membrane potential of the U937 cells (Figure 2C).

To confirm that nHuGzmA was noncytotoxic, we determined the influence of the tryptase on proliferative capacity at 48 hr. Jurkat cells were treated with described concentrations of nHuGzmA, rHuGzmA, or nHuGzmB in presence of HuPFN for 3 hr. Then, cells were cultured for 48 hr, and the number of viable cells was determined. Cells exposed to nHuGzmB and HuPFN showed a dramatic reduction in viability (~20%) at 3 hr and failed to proliferate (Figure 2D and Figure S1). In comparison, cells treated with nHuGzmA or rHuGzmA and PFN were viable at 3 hr (>90%; Figure 2D) and appeared to proliferate unhindered up to 48 hr (Figure 2D and Figure S1).

Nanomolar concentrations of GzmA were used for the reported experiments. The rationale for this depended on the following. GzmA is bound and internalized by target cells at nanomolar concentrations. Furthermore, the delivery agents, HuPFN and AD, readily deliver GzmB intracellularly at similar nanomolar concentrations to induce apoptosis. In contrast, the cytotoxic effect of rHuGzmA has been reported to require micromolar concentrations of the protease (Beresford et al., 1999a), as opposed to nanomolar concentrations used for GzmB-induced apoptosis. The capacity of 1 μM of the native HuGzmA to induce cell death therefore was evaluated in separate experiments with Jurkat and U937 cells. Mitochondrial depolarization, membrane damage (propidium iodide [PI] uptake; data not shown), viability at 48 hr (Figure 2E), ssDNA strand nicks (Figure 2F), and proliferative response at 48 hr (Figure S1C) showed that Jurkat cells were unaffected by the higher concentration of the nHuGzmA in the presence of a concentration of HuPFN that readily delivered GzmB. U937 cells were similarly resistant (Figure S1Div).

In an effort to strictly verify previous work (Beresford et al., 1999a), we treated Jurkat cells with rHuGzmA or nHuGzmA (1 μM) plus rat PFN. Under these conditions, both native and recombinant HuGzmA appeared to augment the effects of rat PFN, inducing membrane damage within 5 min of treatment (Figure 2G), with the recombinant form being more potent. Depending on the permeabilizing concentration of rat PFN, the percentage of damaged cells varied from 50% to 100%. We then discovered that this membranolytic phenomenon occurs not only with active HuGzmA, but also with nHuGzmB and inactive rHuGzmA (Figure 2H). Employing three different cell lines, two separate delivery systems, and three short-term parameters of cell death, as well as a cell-survival assay, we found that HuGzmA failed to manifest an obvious cytotoxic response in presence of nHuPFN. In contrast, micromolar concentrations of the granzyme, either active or inactive, clearly synergized with rat PFN in vitro to induce Jurkat cell to undergo extremely rapid necrosis, as opposed to apoptotic cell death.

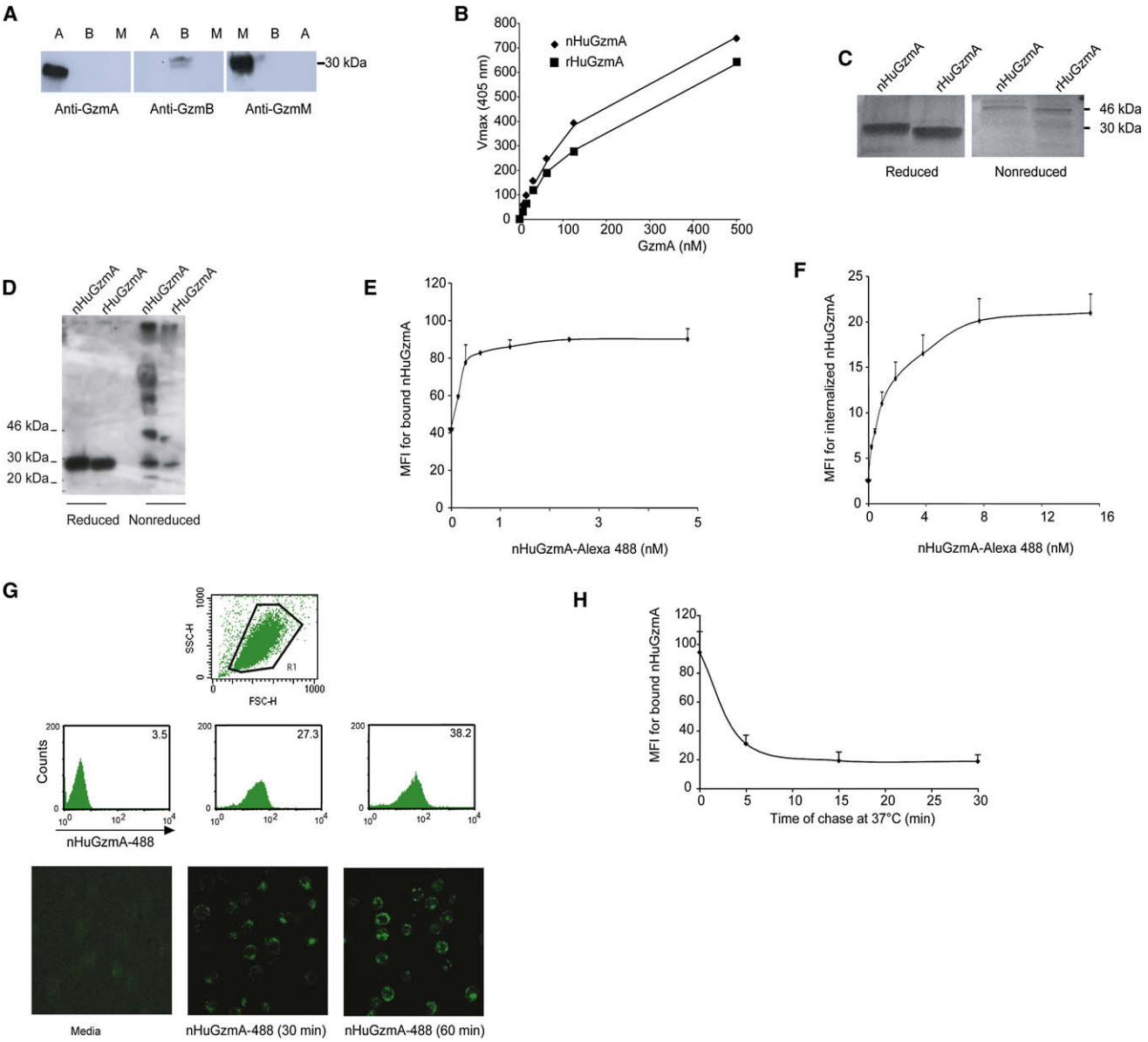


**Figure 1. Characterization of nHuGzmA and rHuGzmA**

(A) nHuGzmA is not contaminated with GzmB or GzmM. Immunoblots of native granzyme A, B, and M (100 ng) were exposed to GzmA (left), GzmB (center), or GzmM (right) Abs.

(B) nHuGzmA is enzymatically active. Esterolytic activities of the native and recombinant human GzmA were measured at the indicated concentrations with standard BLT-esterase assay.

(C and D) nHuGzmA is predominantly dimeric. Reduced and nonreduced nHuGzmA were run on 10% SDS-PAGE and silver stained (500 ng per lane). (D) shows an immunoblot with polyclonal anti-GzmA (100 ng per lane).

(E) nHuGzmA binds to Jurkat cells. Jurkat cells were exposed to nHuGzmA-Alexa 488 at 4°C, washed, and sequentially reacted with Rabbit anti-Alexa 488 and donkey anti-rabbit Alexa 488. Mean fluorescence intensity (MFI, geometric mean) of nHuGzmA binding was plotted against the indicated concentrations (mean ± SD, n = 2). The MFIs (mean ± SD) for autofluorescence and the isotype control were 41.5 ± 0.9 and 41.2 ± 3.0, respectively.

(F) nHuGzmA internalization in Jurkat cells. Targets were incubated with indicated concentrations of nHuGzmA-Alexa 488 for 30 min, washed, and analyzed on the flow cytometer (MFI ± SD, n = 2).

(G) nHuGzmA internalization in Jurkat cells. Cells were incubated with 38.5 nM of nHuGzmA-Alexa 488 for 30 or 60 min, washed, and analyzed by flow cytometry (upper panel) or by confocal microscopy (lower panel).

(H) Clearance of nHuGzmA from plasma membrane. Jurkat cells were exposed to 1.92 nM nHuGzmA-Alexa 488 at 4°C, washed, and then chased at 37°C for varying times with media. Cells were then sequentially reacted with rabbit anti-Alexa 488 and donkey anti-rabbit Alexa 488. MFI of nHuGzmA binding was plotted against the time of chase at 37°C (MFI ± SD, n = 3).

### Do Nanomolar Concentrations of nHuGzmA Synergize with nHuGzmB to Induce Apoptosis?

Although HuGzmA did not appear to be toxic in the presence of sublytic HuPFN, the tryptase might synergize with GzmB to kill target cells. Before addressing this question, however, we evaluated the joint interaction of the proteases with target cells. We designed experiments to investigate whether the two Gzms crosscompete for binding and internalization in our model target cells. Equivalent or higher concentrations (w/w) of unlabeled nHuGzmA efficiently blocked binding of $nHuGzmB_{488}$ to Jurkat cells (Figure 3A). The binding of $nHuGzmA_{488}$ then was evaluated in the presence of unlabelled nHuGzmA, rHuGzmA, and nHuGzmB (Figure 3B). Here, both native Gzms inhibited binding at equivalent levels, but recombinant HuGzmA poorly inhibited nHuGzmA binding. Given the distinct behavior of rHuGzmA, the interaction of labeled rHuGzmA then was assessed. The experiments showed that $rHuGzmA_{488}$ displayed an affinity for Jurkat cells similar to that displayed by nHuGzmA (Figure 3C), but the rate and overall amount of internalized rHuGzmA was substantially less (Figure 3D). The result here suggests that the two native granzymes share common binding site(s) that differ for the recombinant protein and that nHuGzmA might potentially decrease nHuGzmB-induced apoptosis. Considering this information, we then examined potential synergy (or inhibitory effects) between nanomolar levels of nHuGzmA and nHuGzmB. Surprisingly, an excess of nHuGzmA neither increased nor decreased the magnitude of GzmB-mediated apoptosis in the presence of HuPFNPFN (Figure 3E).

### Is Mouse GzmA Cytotoxic In Vitro?

Given the results for HuGzmA, we asked whether MuGzmA might also lack cytotoxic activity. The Henkart lab reported (Hayes et al., 1989) that nMuGzmA, isolated from CTLs, and MuPFN induced both $^{51}Cr$ and $^{3}H$-thymdine release from murine target cells. More recently, P. Bird and colleagues observed that rHuGzmA was not cytotoxic, whereas rMuGzmA and recombinant HuPFN were shown, in preliminary studies, to reduce target cell survival (Cr release and MTT assays) (Kaiserman et al., 2006). We therefore examined whether nMuGzmA and rMuGzmA were cytotoxic in short-term as well as proliferation assays. To proceed, we had to ensure that MuGzmA expressed high enzymatic activity. A direct comparison of mouse and human GzmA is not possible because the proteases have different subsite preferences (Fruth et al., 1987). However, when tested on a relevant substrate, both nMuGzmA and rMuGzmA showed comparable enzymatic activities (nMuGzmA: $37 \times 10^4$ U/nM; rMuGzmA: $48 \times 10^4$ U/nM) (see Figure S4). Delivering these active proteases into EL-4 cells with SLO did not alter the following parameters: PI, annexin, or ROS (Figures 4A and 4B). Furthermore, the potential antiproliferative effect of nMuGzmA was examined in two separate approaches: (1) delivery of nMuGzmA by SLO or HuPFN into EL-4 cells and measuring cell survival by $^{3}H$-Thymidine incorporation (Figure 5A) and (2) treatment of Jurkat cells with nMuGzmA and HuPFN and measuring cell numbers at 48 hr (Figures 5A and 5B). In both instances, neither nMuGzmA nor rMuGzmA significantly affected cell viability or suppressed proliferation of the cell lines. As before, both nHuGzmB and rMuGzmB were able to kill EL-4 targets and inhibit proliferation.

### HuGzmA Induces a Discrete Set of Proinflammatory Cytokines in Adherent Human PBMC

Because HuGzmA appears to lack cytotoxic activity except under restricted conditions that results in rapid necrosis, what might be the biologic function(s) of the protease? We had previously reported that active dimeric nHuGzmA induces expression of proinflammatory-cytokine genes, primarily in human monocytes (adherent PBMC) (Sower et al., 1996a; Sower et al., 1996b).

Our first goal was to perform a more detailed analysis to validate the cytokine profile that GzmA induces in monocytes. Using a multiplex approach, we determined the ability of nHuGzmA to stimulate 14 cytokines: IL-1β, IL-2, IL-4, IL-5, IL-6, IL-8, IL-10, IL-12 (p40 and p70), IL-13, IFN-γ, TNF-α, IP-10, and MIP-1b. Adherent PBMCs were treated with nHuGzmA (10 μg/ml, 192 nM) for 8 hr in the absence of delivery agents. The nHuGzmA induced secretion of substantial amounts of IL-1β, IL-6, and TNF-α (Figure 6A) (IL-8 was also induced; data not shown). Because the cytokine response attributed to nHuGzmA might be due to endotoxin contamination, we excluded this possibility by exposing the protease to an EndoTrap matrix designed to adsorb lipopolysaccharide (LPS). The processed nHuGzmA stimulated amounts of IL-1β, TNF-α, and IL-6 similar to those stimulated by untreated protease, indicating that endotoxin contamination was not a critical factor (Figure 6B). To determine whether cytokine induction required intact enzyme, we evaluated active and inactive rHuGzmA after endotoxin removal. Only active rHuGzmA induced a cytokine response (Figure 6C). Comparison of treated and untreated active HuGzmA indicated that contaminating endotoxin contributed, though only marginally, to the activity of the tryptase (~100 pg/ml of endotoxin is sufficient to induce cytokine secretion by the adherent PBMC; data not shown).

How GzmA signals cytokine induction is unclear (Sower et al., 1996a). Putative receptors that bind and internalize the granzymes (e.g., MPR and plasma-membrane-associated HSPGs and CSPGs) (Motyka et al., 2000; Raja et al., 2005) lack obvious transmembrane signaling motifs. Although nHuGzmA and nHuGzmB are internalized, in part, through shared binding site(s) (see above), only the former appears to induce cytokine expression (Sower et al., 1996a). The possibility therefore exists that nHuGzmA requires internalization and release to the cytosol to signal proinflammatory-cytokine gene expression. We initially addressed this issue by asking whether dimeric nHuGzmA was more active than the monomer. The rationale was that the dimer would be more membranolytic at acidic endosomal pH and thus released to the cytosol in greater quantities. On a molar basis, the dimer was indeed four times more active than the monomer (Figure 7A). For further evidence that GzmA signals intracellularly, rHuGzmA-TAT was expressed, depleted of endotoxin, and added to adherent PBMC. Recombinant HuGzmA-TAT induced a marked increase in both IL-β and TNF-α expression, suggesting that granzyme likely signals within the cytosol to induce the proinflammatory cytokines (Figure 7B).

Because nHuGzmA appears to differentially induce IL-1β, IL-6, and TNF-α in adherent PBMC after cytosolic entry, we speculated that the tryptase might modulate intracellular pathogen-recognition systems. Three main families of pathogen-recognition molecules cooperate in host defense: TLRs, nucleotide-binding

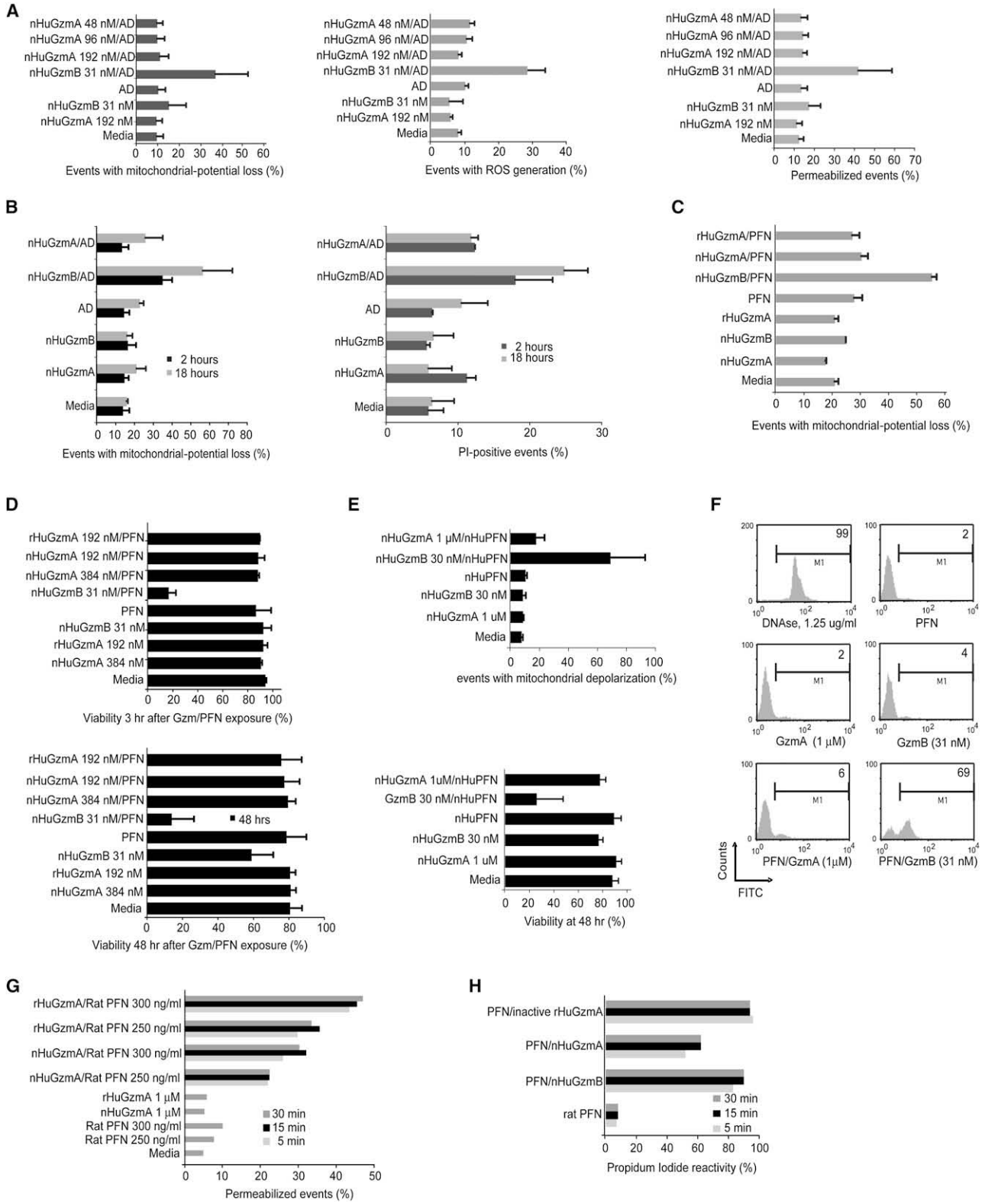


**Figure 2. Human GzmA Does Not Kill In Vitro except under Restricted Conditions**

(A) Jurkat cells were treated with the nHuGzmB or nHuGzmA plus AD for 90 min. Cells were split, and the following were assessed: mitochondrial-potential loss, ROS generation, and cell viability (mean ± SD, n = 3).

oligomerization domain (NOD)-like receptors (NLRs), and retinoid acid-inducible gene-1 receptors. The NLRs, in turn, can be divided into two distinct pathways that act through peptidoglycan molecules or muramyl peptides versus IPAF or Cryopyrin (Franchi et al., 2006). For the latter, a fundamental upstream signal involves activation of the proinflammatory caspase-1. Using the specific caspase-1 inhibitor WEHD-FMK and the pan-caspase inhibitor ZVAD-FMK, we investigated whether nHuGzmA-mediated induction of IL1-β, TNF-α, and IL-6 was associated with intracellular caspase-1 activation. Native HuGzmA stimulated adherent PBMC to produce a robust IL-1β, TNF-α, and IL-6 response that was almost completely blocked by WEHD-FMK, as well as by the pan-caspase inhibitor (zVAD-fmk) (Figure 7C).

We then evaluated whether intact cytotoxic cells that selectively secrete GzmA might, together with PFN, induce human adherent PBMC to produce the identified proinflammatory cytokines. To answer this question, we added a NK92 subline (Maki et al., 2001) to adherent cells in the presence and absence of EDTA to block granule secretion, and the cytokine response was determined at 6 hr. The results for this model system suggest that NK92 cells induce the adherent cells to secrete IL-1β (Figure 7D) and TNF-α (data not shown).

### MuGzmA and GzmA from Mouse CTL Induce IL-1β from Primary Mouse Macrophages

To learn whether the phenomenon observed for HuGzmA was species specific, we evaluated the cytokine-inducing capacity of isolated rMuGzmA and CTLs expressing the protease. LPS-activated, adherent peritoneal macrophages were treated with rMuGzmA and sublytic SLO or with ATP (Figure 7E, positive control) for 3 hr. Recombinant MuGzmA delivered by SLO induced a dose-dependent increase in IL-1β (Figure 7E), whereas inactive rMuGzmA (PFR-CK pretreated) was ineffective (data not shown). Next, to learn whether the secretion of IL-1β is also induced by GzmA positive CTL, we incubated LPS-stimulated adherent peritoneal macrophages with ex vivo-derived or in vitro-propagated LCMV-immune *Gzmb*$^{-/-}$ CTL ± virus-specific peptide gp33 for 3 hr. LCMV-immune *Gzmb*$^{-/-}$ CTL specifically induced IL-1β-release in a dose-dependent manner under the described conditions (Figure 7E).

### Biological Relevance of GzmA to a Systemic Inflammatory Response

To assess the biological relevance of gzmA to inflammatory processes in vivo, we evaluated the susceptibility of WT and Gzm-deficient mice to LPS-induced mortality. Compared to WT mice, *Gzma*$^{-/-}$ mice were more resistant to challenge with LPS (Figure 7F). Remarkably, *Gzmb*$^{-/-}$ mice manifested greater resistance, whereas *Gzma*$^{-/-}$*Gzmb*$^{-/-}$ mice were as susceptible to LPS as WT mice, suggesting that both GzmA and GzmB contribute to LPS-associated inflammatory processes in vivo.

## DISCUSSION

Our unanticipated results suggest that human and mouse GzmA are not toxic in the presence of vehicles (PFN, AD, and SLO) that facilitate their intracellular delivery except under very restricted, nonphysiologic conditions. Instead, active, endotoxin-free nHuGzmA and rMuGzmA appear to activate the innate immune response by inducing key proinflammatory cytokines. The cytokine response appears to be relatively selective for monocytic-like cells, involves cytosolic localization of GzmA, and is induced by isolated human and mouse GzmA, as well as by human NK cells and murine CTLs that selectively secrete the granzyme. Together with the results showing that GzmA contributes to the lethal effects of LPS, the data strongly support the concept that the granule-secretion pathway modulates inflammatory processes as well as mediates cell death.

Since their original description, we have all operated under the supposition that the granzymes would have cytotoxic activity. This concept was established for GzmA when MuGzmA and MuPFN were noted to induce cell death after addition to suspended target cells (Hayes et al., 1989). In similar work, the Greenberg lab then reported that isolated nRatGzmA was cytotoxic in the presence of rat PFN. During cation-exchange chromatography to isolate the native proteases from cytotoxic granules, GzmA and GzmB elute sequentially in overlapping peaks. A sensitive GzmB substrate (or EIA) was not available to ensure GzmA was free of contaminating GzmB. Thus, the apparent cytotoxicity of the mouse and rat GzmA might be due to contamination of the isolated tryptase with coeluted GzmB (unpublished data).

(B) HeLa cells were treated with nHuGzmA (192 nM) or nHuGzmB (31 nM) plus AD for indicated times. Mitochondrial-potential loss or cell viability were investigated (mean ± SD, n = 3).
(C) U937 cells were treated with nHuGzmA or rHuGzmA (both 192 nM) or nHuGzmB (31 nM) plus PFN (100 ng/ml) for 2 hr at 37°C. Cells were stained with CMX-ROS for evaluation of mitochondrial depolarization (mean ± SD, n = 3).
(D) Jurkat cells were treated with nHuGzmA (384 nM or 192 nM), rHuGzmA (192 nM), or nHuGzmB (31 nM) plus PFN for 3 hr, and cell viability was determined by trypan blue stain. Cells were then washed and replated for 48 hr, and viability was measured (mean ± SD, n = 3).
(E) The effects of high-dose GzmA on Jurkat cells. Jurkat cells were treated with nHu GzmA (1 μM) or nHuGzmB (31 nM) plus a subpermeabilizing concentration of nHuPFN (125 ng/ml) for 90 min. Mitochondrial-potential loss was assessed (top panel) at 90 min. A parallel set was incubated for 3 hr, washed, and replated for 48 hr, and viability was measured (bottom panel) (mean ± SD, n = 3).
(F) Jurkat cells were treated with nHu GzmA (1 μM) or nHuGzmB (31 nM) plus a subpermeabilizing concentration of nHuPFN (125 ng/ml) for 180 min, and ssDNA nicking was determined by flow cytometry (FCM). Cells treated with DNAase (1.25 μg/ml, 20 min at room temperature) served as a positive control. Data are representative of two independent experiments.
(G) Jurkat cells were treated with either nHu GzmA or rHuGzmA (1 μM) plus subpermeabilizing concentrations of rat PFN (250 and 300 ng/ml) for times ranging from 5 to 30 min, and membrane damage was determined by PI and FCM. Data are representative of two independent experiments.
(H) Jurkat cells were treated with rat PFN and the described granzyme preparations for times indicated. Propidium iodide was added at the end of the incubation period, and cells were then analyzed by FCM. PI reactivity is defined as fluorescence activity exceeding $10^3$ units (log scale). Concentration of each granzyme protein was 1 μM.

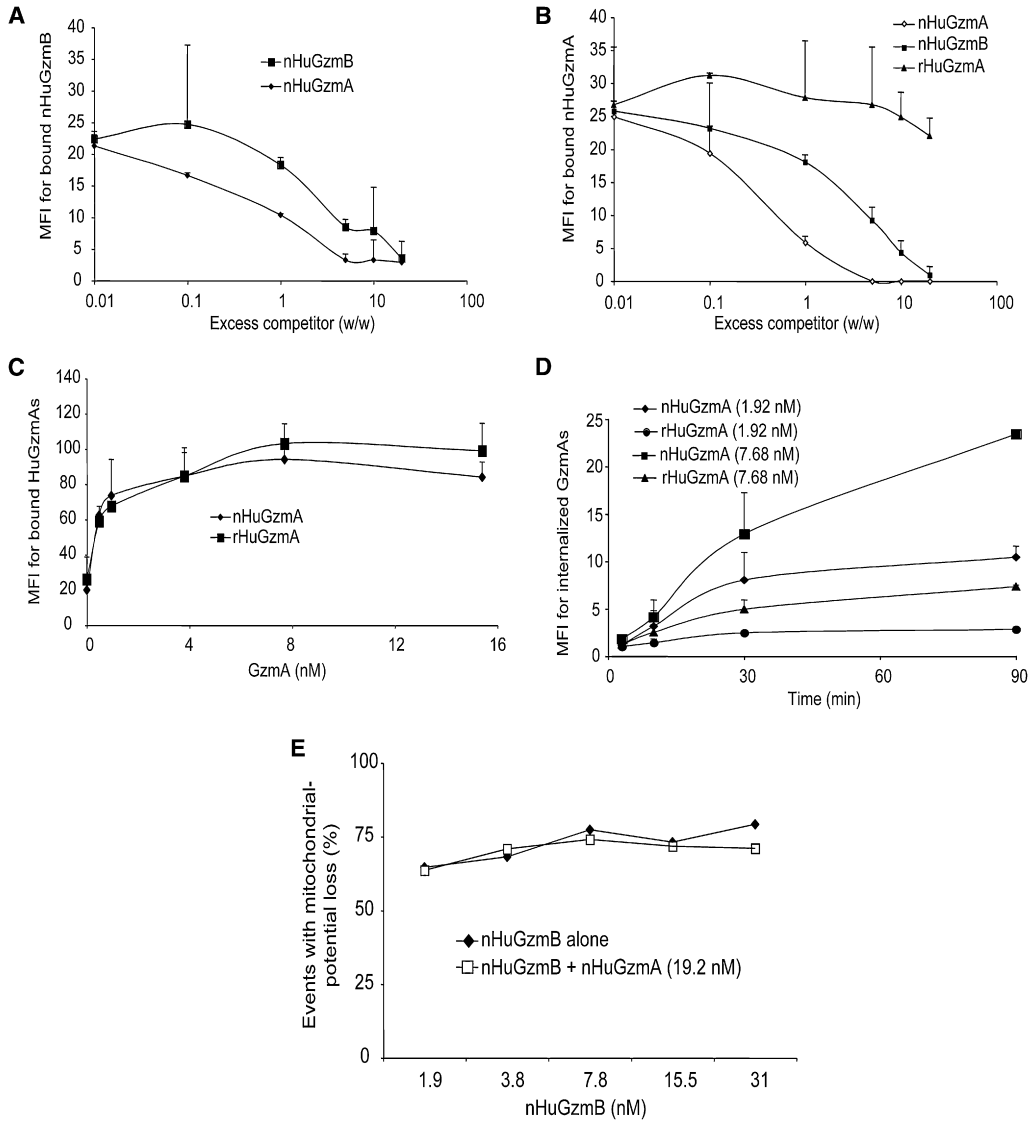


**Figure 3. nHuGzmA Competes with nHuGzmB for Binding Sites on Jurkat Cells**

(A) Jurkat cells were incubated with $nHuGzmB_{488}$ (0.78 nM) plus either nHuGzmA or nHuGzmB ranging in concentrations from 0.01- to 20-fold excess (w/w) on ice for 30 min, followed by measurement of granzyme binding (mean MFI ± SD, n = 2).

(B) Jurkat cells were incubated with $nHuGzmA_{488}$ (0.48 nM) in the presence of nHuGzmA, nHuGzmB, or rHuGzmA from 0.01- to 20-fold excess (w/w) on ice for 30 min, followed by measurement of granzyme binding (mean MFI ± SD, n = 2).

(C) nHuGzmA and rHuGzmA bind to Jurkat cells with similar affinity. Cells were exposed to either the $nHuGzmA_{488}$ or the $rHuGzmA_{488}$ at 4°C, followed by measurement of granzyme binding (mean MFI ± SD, n = 3).

(D) nHuGzmA is internalized more rapidly than rHuGzmA by Jurkat cells. Targets were incubated with indicated concentrations of $nHuGzmA_{488}$ or $rHuGzmA_{488}$ for the indicated times, washed, and analyzed on the flow cytometer (MFI ± SD, n = 2).

(E) nHuGzmA does not augment nHuGzmB-induced apoptosis. Jurkat cells were incubated with nHuGzmB (1.9 nM to 31 nM) and sublytic concentration of PFN (25 ng/ml) in the absence or presence of nHuGzmA (19.2 nM) for 90 min at 37°C. Mitochondrial-membrane potential was then investigated (representative data for one of two experiments). Mitochondrial-potential loss in samples treated with nHuGzmA and PFN was 19.3 ± 5 (mean ± SD).

The Lieberman lab has reported biochemical events surrounding GzmA-induced cell cytotoxicity with the combination of rHuGzmA and rat PFN (Beresford et al., 1999a; Fan et al., 2003a; Fan et al., 2002; Fan et al., 2003b; Martinvalet et al., 2005; Zhang et al., 2001; Zhang et al., 2003). We show here that a mixture of micromolar HuGzmA and rat PFN causes virtually instantaneous membrane permeabilization, the time frame of which suggests that the granzyme somehow augments the membranolytic action of PFN. Notably, active and inactive rHuGzmA both induce $^{51}Cr$ release (Beresford et al., 1999a; see also Beresford et al., 1999b). This observation is consistent with data here showing active and inactive HuGzmA and active HuGzmB all induce rapid membrane damage with rat PFN.

How might micromolar amounts of granzyme enhance the membranolytic effects of PFN? We have observed that limited concentrations of minimally permeabilizing rat PFN induce

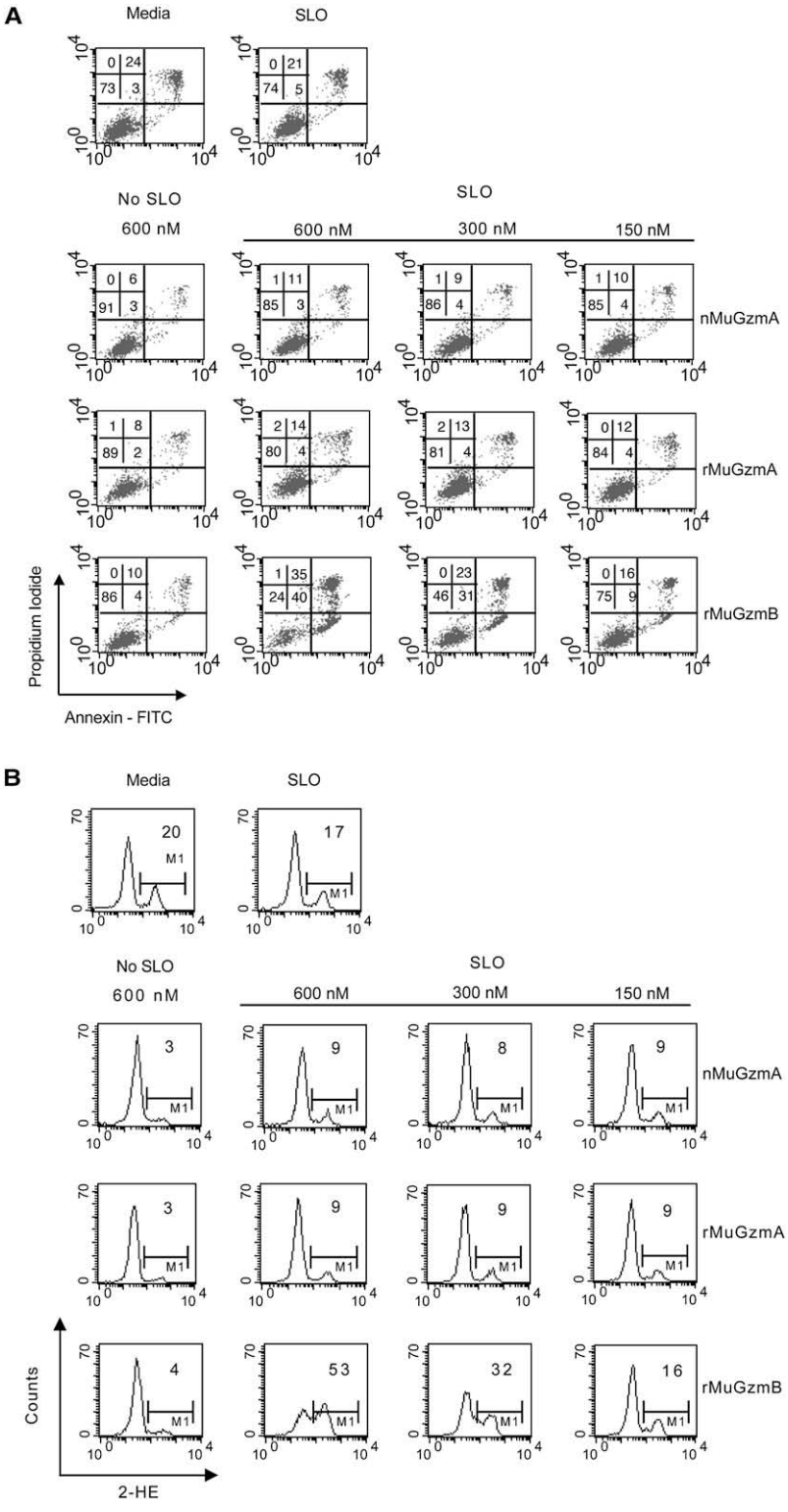


**Figure 4. nMuGzmA and rMuGzmA Are Not Cytotoxic as Determined by Multiple Parameters**

Analyses of apoptotic parameters during nMuGzmA- and rMuGzmA-induced cell death in EL4 cells. EL4 cells were incubated with the indicated amounts of protease in the presence or absence of a sublytic dose of SLO for 4 hr or were left untreated (control). PS translocation (A; annexin V staining), membrane damage (A; PI incorporation), and ROS generation (B) were analyzed by FACS. See table (inset) for summarized data from three to five experiments.

a subset of low-PI reactive cells (mean fluorescence intensity [MFI]: 10–100) when PI (10 μg/ml) is added simultaneously with PFN. This PI uptake, which appears to consist of endocytic and trans-pore entry of the fluorophore (data not shown), seems to be a prerequisite for the observed membrane damage produced by the micromolar concentrations of granzyme (data not shown). Comprehensive titration reveals that restricted amounts of HuPFN also produce this low-PI reactivity. Such concentrations synergize with micromolar concentrations of HuGzmA to enhance membrane damage, indicating that the phenomenon is not unique to rat PFN (data not shown).

Although the basis for this phenomenon awaits analysis, we speculate that the density of the transient pores formed by PFN must first exceed a critical threshold at which integral proteins cluster, encouraging increased focal binding of the granzyme and consequent membrane disruption. Overall, GzmA does not manifest cytotoxic activity in vitro except under unique conditions in which relatively high concentrations of HuGzmA and restricted concentrations of rat or HuPFN are used. In this instance, the ensuing cell death is clearly necrotic and not consistent with CTL-mediated apoptosis in vitro (Goldberg et al., 1999; Hu and Kipps, 1999). Consequently, many of the observed biochemical events associated with GzmA-induced cell cytotoxicity in vitro may entail the effect of the protease on dead cells.

The studies involving isolated human and mouse GzmA seem to contradict data reported for cytotoxic cells. For example, GzmA$^+$ CTLs (*Gzmb*$^{-/-}$ mice) kill EL4 cells, albeit with considerably less potency than GzmB$^+$ CTL (*Gzma*$^{-/-}$ mice) (Pardo et al., 2004). This observation corresponds with earlier work in which the coexpression of MuGzmA and MuPFN genes endow RBL cells with the capacity to induce $^{51}$Cr release and DNA fragmentation in EL4 cells (Shiver et al., 1992). However, the cytotoxic potential of GzmA in CTL and transfected RBL may not be due to the protease per se, but depend instead on additional molecules present in cytoplasmic granules (e.g., other Gzms and/or cathepsins). In this regard, ex vivo-derived virus-immune CTL from wild-type and *Gzmb*$^{-/-}$ mice, retrieved at the peak of their cytotoxic response, express GzmK transcripts and protein (Pardo et al., 2008; unpublished data). Although the inconsistencies observed between the cytotoxic activity of

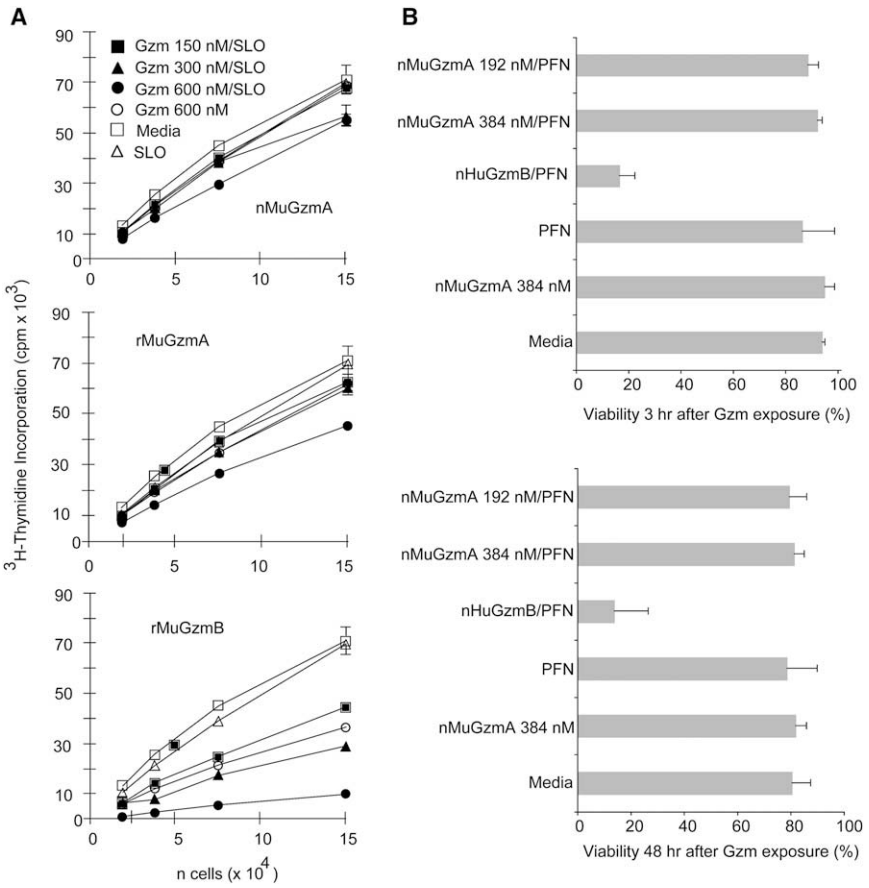


**Figure 5. nMuGzmA Is Not Cytotoxic as Determined Proliferative Assays**

(A) Analysis of granzyme cytotoxicity in EL4 cells by a survival assay. EL4 cells were incubated with the indicated amounts of nMuGzmA or rMuGzmA in the presence or absence of a sublytic SLO for 4 hr. After washing, cell survival was monitored by $^{3}$H-thymidine incorporation as described in the Experimental Procedures. A representative experiment of two independent experiments is shown.

(B) Analyses of nMuGzmA cytotoxicity in Jurkat cells by 48 hr viability assay. Jurkat cells were treated with nMuGzmA (384 nM or 192 nM) or nHuGzmB (31 nM) plus PFN for 3 hr, and cell viability was determined by trypan blue stain (top panel). Cells were then washed and replated for 48 hr, and viability was measured (bottom panel) (mean ± SD, n = 3).

isolated granzymes and effector cells may be simply methodological, further evaluation is necessary for clarification of the paradoxes.

The data described here support the proposal that the granule-secretion pathway modulates inflammatory reactions with GzmA and perhaps other granzymes as key participants. Whether GzmA contributes to proinflammatory responses as well as indirectly to cytotoxic responses now merits consideration. Supporting a role in noncytotoxic, antipathogen host defense is the fact that Gzma$^{(-/-)}$ mice are known to succumb to viral pathogens such as ectromelia (Mullbacher et al., 1996). In this instance, GzmA may trigger virally infected cells to produce cytokines, attracting phagocytes to clear the infection. Could GzmA mediate a similar noncytotoxic function in antitumor immunity? In the case of tumor control, secreted GzmA may induce nonspecific host defense mechanisms, even if the targets are refractory to CTL-mediated apoptosis. Although our limited efforts suggest that monocytic cells (Sower et al., 1996a; Sower et al., 1996b) as well as murine peritoneal macrophages are most receptive to the effects of GzmA, it will be intriguing to learn whether GzmA might also induce tumor cells to produce bioactive molecules that encourage their elimination. Thus, the identification of the range of the responsive cells in both mouse and man requires additional effort, especially in regards to whether the cytokine-inducing properties of GzmA contribute indirectly to granule-mediated apoptosis of tumor cells.

Beside the potential host defense benefits of GzmA, the protease could contribute to immunopathology (Simon et al., 1993). Recent work has shed light on the role of granzymes in the immunopathology of mCMV infection (van Dommelen et al., 2006). PFN$^{-/-}$ mice succumb to inoculated virus, whereas GzmAxB$^{-/-}$ mice survive. Infected PFN-deficient mice develop the Hemophagocytic Syndrome (HS), a state of cytokine hypersecretion combined with marked proliferation in T cells and monocytes. The clinical equivalent of HS occurs commonly in patients with connective-tissue diseases (Dhote et al., 2003), as well as in patients who have defects in the granule-secretion pathway (Menasche et al., 2005). Importantly, TNF-blocking Ab attenuated the intensity of the immunopathology in the PFN$^{-/-}$ mice, establishing a causal role for the cytokine in mediating this hyperactive inflammatory state. Given that we have not observed a consistently robust induction of proinflammatory cytokines by cells exposed to GzmB, the results from the Degli-Espoti group (van Dommelen et al., 2006) suggest that GzmA might contribute to the development of at least one form of HS.

Although the data indicate that GzmA-mediated cytokine induction is, in part, caspase-1 dependent, the understanding of the signaling mechanism is highly speculative. Our past efforts have focused on determining whether GzmA triggers gene expression via a transmembrane signal. The tryptase, however, fails to induce Ca influx to efficiently cleave various PAR subtypes, and it fails to stimulate linked kinase activity (ERK-1) (data not shown). Tschopp et al. have reported that murine GzmA directly matures IL-1β, and the processed cytokine is detectable in targets attacked by murine CTLs (Irmler et al., 1995). We have been unable to reproduce maturation of human IL-1β by treating lysates of THP-1 cells with nHuGzmA, suggesting the existence of alternate mechanisms that might be species specific. The involvement of caspase-1 in GzmA-mediated IL-1β production offers a vital clue, however, to the mechanism underlying signaling by the granzyme. Virtually all the described

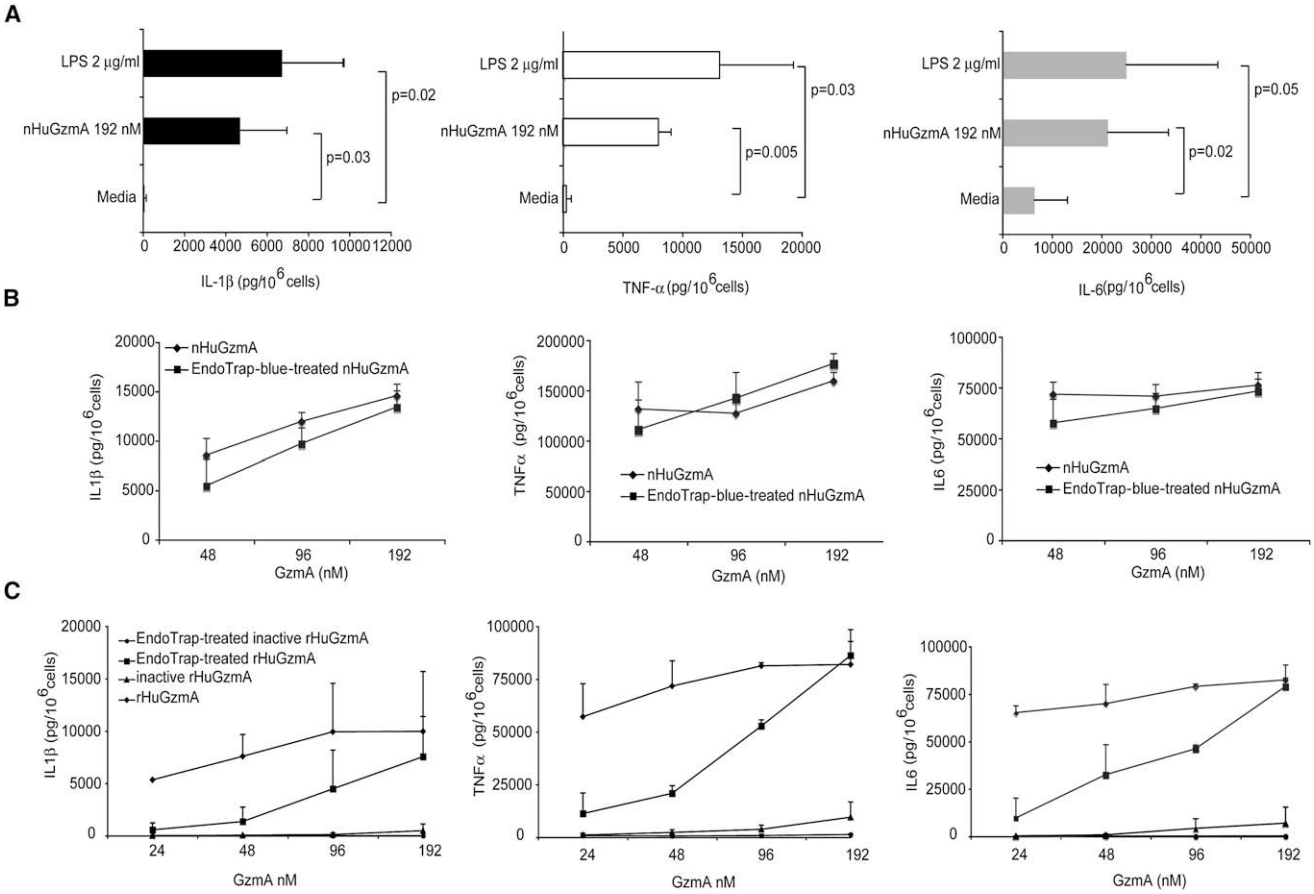


**Figure 6. nHuGzmA Elicits a Proinflammatory Cytokine Response**

(A) Adherent PBMCs were treated with nHuGzmA (192 nM) or LPS (2 μg/ml) for 8 hr at 37°C, and supernatants were evaluated in a cytokine multiplex array that measures 14 cytokines simultaneously. Three cytokines, IL-1β, IL-6, and TNF-α, were upregulated after GzmA treatment. Results are represented as mean ± SD of three normal donors. p value was determined with a paired Student's t test.

(B) Endotoxin-free nHuGzmA induces human monocytes to secrete IL-1β, TNF-α, and IL-6. nHuGzmA, depleted of potentially contaminating endotoxin with EndoTrap matrices, was added to adherent PBMC for 8 hr, and supernatants were assayed for IL-1β, TNF-α, and IL-6. Cytokine concentration for media control was consistently 0 pg/million cells. For LPS-treated cells, the values for IL-1β, TNF-α, and IL-6 were respectively 40,000 ± 9,000, 28,0000 ± 60,000, and 195,000 ± 32,000 pg/million cells. (Data represent mean ± SD for three normal donors.)

(C) IL-1β, TNF-α, and IL-6 production in adherent PBMC requires active GzmA. Proteolytically active and inactive rHuGzmA (S195A) and their corresponding endotoxin-depleted samples were added to adherent PBMCs for 6 hr, and supernatants were assayed for IL1β, TNF-α, and IL-6. Cytokine concentration for media control was consistently 0 pg/million cells. For LPS-treated cells, the values for IL-1β, TNF-α, and IL-6 were respectively 16,000 ± 9,000, 141,000 ± 7,500, and 115,000 ± 24,000 pg/million cells. (Data represent mean ± SD for three normal donors.)

pathways linking caspase-1 and IL-1β involve the phenomenon of pattern recognition, a multiprotein oligomerization process that results in the activation of proinflammatory caspases and IL-1β (e.g., the inflammasome) (Martinon, 2007). The data reported here suggest that GzmA may be an important component of the granule-secretion pathway linking innate and adaptive immune responses to inflammatory cascades.

## EXPERIMENTAL PROCEDURES

### Cell Lines

Jurkat, U937, HeLa, and K562 cells were maintained in complete RPMI media. NK92 cells (a kind gift from G. Maki, University of Illinois at Chicago) were grown in Myelocult media (GIBCO Tech). The murine thymoma cell line EL4.F15 has been described (Pardo et al., 2002).

### Reagents

nHuGzmA, nHuGzmB, human PFN, and rat PFN were isolated as described (Froelich et al., 1996; Hanna et al., 1993) (Shi et al., 1992). Recombinant human GzmA (rHuGzmA) was purchased from Axxora or expressed (Beresford et al., 1997). Inactive GzmA was generated by site-directed mutagenesis of the active Ser (Beresford et al., 1997). AD were also used for granzyme delivery (Metkar et al., 2003). nMuGzmA was isolated from the CTL line 1.3E6SN (Simon et al., 1986). Recombinant MuGzmA and rMuGzmB were expressed in *E. coli*. SLO was kindly provided by S. Bakhdi. The nHuGzmA, nHuGzmB, and rHuGzmA were labeled with AlexaFluor488 according to the manufacturer's instructions, and esterolytic activity was tested (see Figure S2).

All reagents and tissue culture supplies were purchased from either Sigma or GIBCO BRL. FITC- and PE-labeled mouse isotype controls, as well as FITC-CD3, FITC-CD19, and FITC-CD56, were from BD PharMingen. The PE-labeled CD14 (Beckman Coulter) was a kind gift from R. Pope (Feinberg School of Medicine, Chicago). Ready gels, silver-stain kit, and Immun-Blot and Sequi-Blot PVDF membranes were purchased from Bio-Rad. ECL

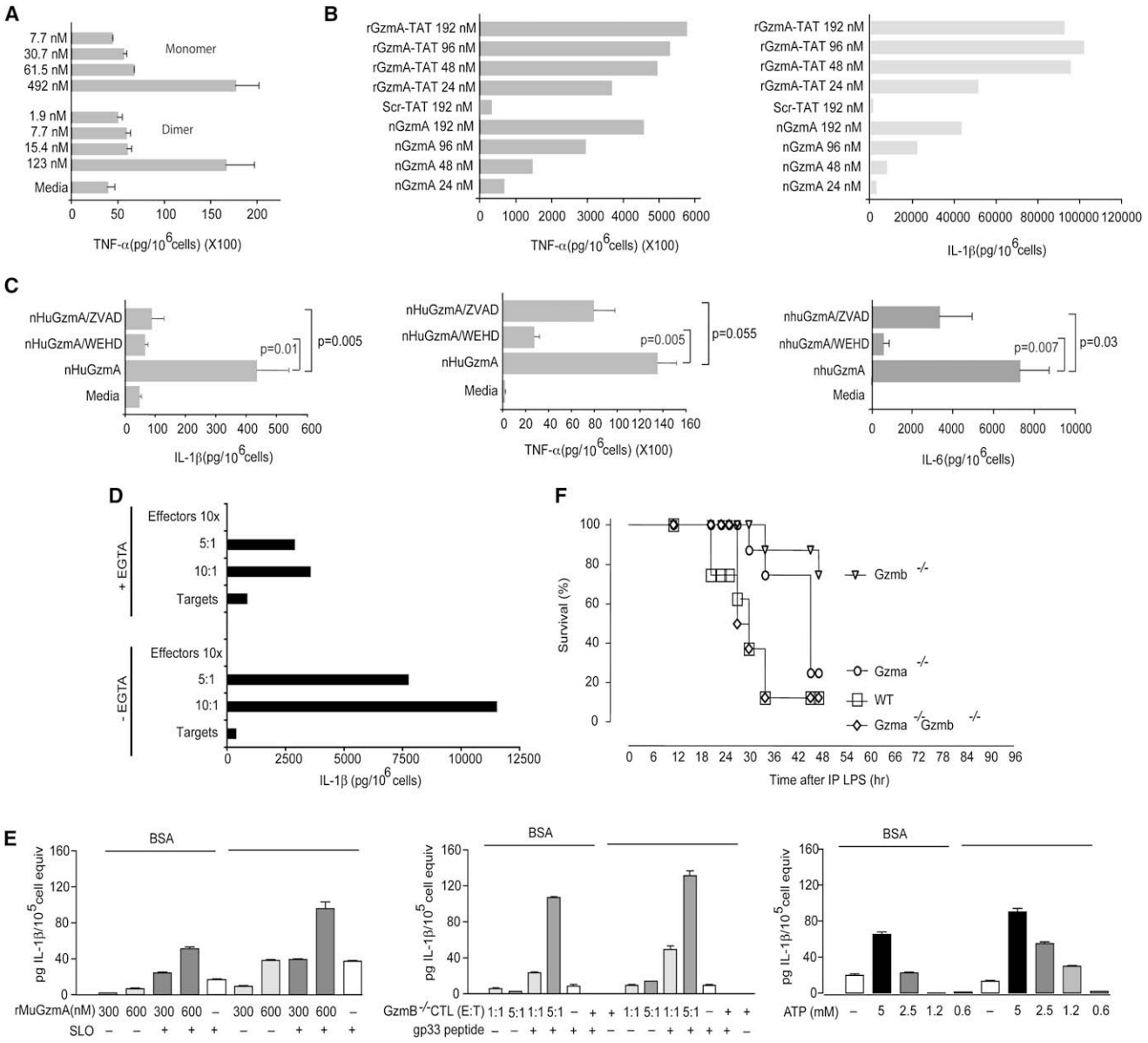


**Figure 7. HuGzmA and MuGzmA Require Intracellular Delivery for Optimal Induction of Cytokine Release**

(A) Dimeric nHuGzmA is a more potent inducer of TNFα than monomeric protease. Monocytes were incubated with dimeric and monomeric nHuGzmA for 8 hr at 37°C, and supernatants were assayed for TNF-α (mean ± SD of two normal donors).

(B) GzmA-TAT is a more efficient inducer of IL-1β and TNF-α than dimeric nHuGzmA. The GzmA-TAT fusion protein was isolated and depleted of endotoxin. The GzmA-TAT was 4.31-fold less active than the nHuGzmA by weight. Equivalent concentrations of the nHuGzmA and GzmA-TAT by weight were added to adherent PBMCs for 8 hr, and supernatants were assayed for IL1β and TNF-α. IL-1β concentration for media and LPS were 0 and 68,000 pg/million cells, respectively. TNFα level in media and LPS were 0 and 660,000 pg/million cells, respectively. An irrelevant SCR-TAT fusion protein (10 μg/ml, 192 nM equivalent) was used as a control for the GzmA-TAT protein. It elicited an IL-1β response of 411 pg/million cells and a TNF-α response of 439 pg/million cells. (Data represent one of two donors.)

(C) nHuGzmA-induced IL-1β, TNF-α, and IL-6 secretion requires caspase-1 activity. Adherent PBMCs were treated with nHuGzmA (192 nM) in media with DMSO as a vehicle control, with caspase-1 inhibitor (WEHD-FMK, 50 μM), or with the pan-caspase inhibitor ZVAD-FMK (50 μM) for 6 hr at 37°C. The supernatants were assayed for IL-1β, TNF-α, and IL-6 ELISA (mean ± SD of three normal donors). p value was determined with a paired Student's t test.

(D) NK92 effectors induce adherent PBMCs to secrete IL-1β. NK92 cells were incubated with adherent PBMC targets at 10:1 and 5:1 ratios for 8 hr at 37°C in the presence or absence of EGTA (10 mM). Supernatants were subjected to EIA, with results representative of four donors. The control to assess the possible influence of EGTA on the adherent cells (nHuGzmA-stimulated cells plus EGTA) showed that the chelator was not directly inhibitory (data not shown).

(E) rMuGzmA induces IL-1β release in primary mouse macrophages. Adherent peritoneal macrophages were incubated with the indicated amounts of rMuGzmA ± SLO (0.5 μg/ml) or ATP for 3 hr, and supernatants were assayed for IL-1β (mean ± SD). LCMV-immune *Gzmb*$^{-/-}$ CTLs specifically induce IL-1β release in primary mouse macrophages. Adherent peritoneal macrophages were incubated with LCMV-immune *Gzmb*$^{-/-}$ CTL at 1:1 and 5:1 ± gp33 for 3 hr, and supernatants were assayed for IL-1β (mean ± SD).

Western blot system and Hyperfilm ECL were from Amersham Pharmacia Biotech.

### BLT-Esterase Assay

The esterolytic activities of GzmAs were measured with the Thiobenzyl benzyloxycarbonyl-L-lysinate substrate (Hanna et al., 1993).

### Immunoblotting

Blotted proteases were probed with anti-GzmA (clone GA-4, 1:1000), anti-GzmB (clone 2C5, 1:10000, from J. Trapani), or anti-GzmM (clone 4H10, 1:1000, from M. Smyth). The blots were developed with a mouse HRP Ab (1:1000, Amersham Pharmacia Biotech) and the ECL kit.

### Production and Isolation of the rHuGzmA-TAT Fusion Protein

A nine aa sequence from HIV-TAT protein (RKKRRQRRR) (Nagahara et al., 1998) was added to the C terminus of GzmA with high-fidelity pfu enzyme, followed by cloning, expression, and isolation as described (Beresford et al., 1997). A control TAT-Scramblase protein (Biotin-AHA-YGRKKRRQRRR-SKLACFSHG-CONH2 with TAT sequence underlined) preceded by an aminohexanoicacid (AHA) spacer was synthesized by Tufts University core facility. Both proteins were subjected to endotoxin depletion (see below), and protein concentrations were determined by Coomassie stain with reduced nHuGzmA as the standard.

### Generation of Monomeric nHu GzmA

Dimeric granzyme was reduced with β-Mercaptoethanol (2-ME, 690 mM) for 30 min at 37°C and dialyzed against PBS. Silver staining and immunoblotting confirmed reduction of the disulfide bonds. The concentration of monomeric granzyme was determined by Coomassie stain and densitometry with reduced nHuGzmA that served as an internal standard. Esterolytic activity of the monomer averaged 90% of the original dimer.

### Internalization, Binding, and Competition and Clearance assays

Internalization, binding, and competition experiments were done essentially as described for nHuGzmB (Raja et al., 2005). For confocal microscopy, cells were allowed to adhere to poly-l-lysine-coated slides, mounted with anti-fade reagent (Molecular Probes), and imaged with a Nikon C1 microscope system under 63× magnification. Images were acquired with the Nikon C1 software.

### Apoptosis Assays

AD, 200 and 4000 Pfu/cell for Jurkat and HeLa cells, respectively, or huPFN (permeabilizing <30% cells) acted as granzyme-delivery agents. Mitochondrial-potential loss was measured as reported (Metkar et al., 2003). ROS generation was measured with Hydroxyethidium (2HE, 2 uM) (Martinvalet et al., 2005). Treatment of cells with hydrogen peroxide served as a positive control for HE staining. Cell viability was measured with propidium iodide (5–10 μg/ml) and flow cytometry or by trypan blue and light microscopy.

For studies of mouse Gzms, EL4 cells were incubated with either AD, a sublytic human PFN, or SLO ± granzymes. After the indicated time frames, propidium iodide incorporation, annexin V staining, mitochondrial-potential loss, and ROS production (2HE) were analyzed by fluorescence-activated cell sorting (FACS) (Metkar et al., 2003; Pardo et al., 2004).

### Measurement of ssDNA Strand Nicking by Flow Cytometry

Assay was performed with the Klenow DNA Frag-EL kit according to the manufacturer's instructions with one modification. In lieu of the of immunohistochemistry approach, FITC-dUTP and flow cytometry were used to measure ssDNA nicks. Cells treated with DNAase (1.25 μg/ml) served as positive controls.

### Proliferation Assay

Jurkat cells were treated with either nHuGzmA, nHuGzmB, or nMuGzmA in the presence of PFN for 3 hr at 37°C. The cells were washed in Eppendorf tubes, viability was measured, and cells were replated in RPMI with 10% fetal calf serum at a density of $1 \times 10^5$ cells in 0.5 ml media per well in a 24-well plate. Cultures were analyzed at 24 or 48 hr for total cell number and viability.

### Thymidine Incorporation

El4 cells ($1 \times 10^5$ cells) were treated with Gzms in the presence or absence of a sublytic dose of SLO for 4 hr. Cells were then plated in 96-well plates in triplicate (200 μl/well), and 0.5 μCi of $^3$H-thymidine was added to each well. After 12 hr, cells were harvested, and incorporated radioactivity was measured.

### Proinflammatory Cytokine Response in Human Adherent PBMC

Human PBMCs were isolated by Ficoll-Hypaque density centrifugation (Sigma). Monocytes were enriched through plastic adherence (Sower et al., 1996a); yields consistently represented 10% of input. The adherent cells were treated with the proteases for 6 to 8 hr at 37°C. The supernatants were collected, and the level of cytokines was measured with a Human Cytokine Microarray Kit (Allied Biotech). The 14 cytokines detected were IL-1β, IL-2, IL-4, IL-5, IL-6, IL-8, IL-10, IL-13, IFN-γ, IP-10, MIP-1β, TNF-α, IL-12 (p40), and IL-12 (p70). In other experiments, TNFα, IL1β, and IL6 were quantitated with ELISA kits from Biosource International (Invitrogen) and R&D Systems.

### Use of Caspase Inhibitors

Adherent cells were treated with nHuGzmA in the presence of solvent (DMSO), a caspase-1-specific inhibitor (Z-WEHD-FMK, 50 μM; R&D systems), or the pan-caspase inhibitor, ZVAD-FMK (EMD Biosciences) for 6 hr. Supernatants were assayed for IL-1β, IL-6, and TNF-α by ELISA.

### Preparation of Endotoxin-Depleted GzmA

NHuGzmA preparations were subjected to endotoxin removal with the EndoTrap-Blue kit (Cambrex Biosciences).

### Induction of IL-1β Release from Primary Mouse Macrophages by Isolated Gzm or Ex Vivo-Generated CTL

Adherent thioglycollate-stimulated macrophage from C57BL/6 mice were prestimulated with LPS (10 ng/ml) for 3 hr. After washing, cells were exposed to rMuGzmA (±SLO, 0.5 μg/ml) for 3 hr in either basal media or with BSA supplement. For select studies, rMuGzmA was inactivated with PFR-CK for 30 min. LPS-prestimulated adherent primary macrophages were incubated with ex vivo-derived or in vitro-propagated LCMV-immune gzmB$^{-/-}$ CTL ± LCMV peptide gp33 for 3 hr (Pardo et al., 2008). Supernatants were tested for IL-β by EIA (Invitrogen). ATP served as positive control.

### NK-92-Induced Cytokine Secretion by Human PBMC Adherent Cells

NK92 cells served as effectors, with adherent PBMC serving as targets, in an 8 hr cytotoxicity assay at two effector: target ratios (10:1 and 5:1) in the presence or absence of EGTA (10 mM). Supernatants were then subjected to cytokine EIA.

### LPS-Induced Mortality in Mice

LPS challenge was carried out with weight- and age-matched C57BL/6 (WT), GzmA$^{-/-}$, GzmB$^{-/-}$, and GzmA$^{-/-}$GzmB$^{-/-}$ mice. Animals were injected intraperitoneally (i.p.) with 27 μg LPS (*Salmonella abortus equi; NG420;* dissolved in PBS) per g body weight. Morbidity and mortality were monitored every 2 hr through the indicated time period. All animal experiments were carried out in accordance with the local animal care commission.

(F) Differential susceptibility of C57BL/6 (WT), *Gzma*$^{-/-}$, *Gzmb*$^{-/-}$, and *Gzma*$^{-/-}$*Gzmb*$^{-/-}$ mice to high doses of LPS. Age-matched C57BL/6 (eight males), *Gzma*$^{-/-}$ (four males, four females), *Gzmb*$^{-/-}$ (five males, 3 females), and *Gzma*$^{-/-}$*Gzmb*$^{-/-}$ mice (5 males, 3 females) were injected i.p. with 27 μg of *Salmonella abortus equi*-derived *LPS*/g body weight, and survival was monitored for 48 hr.

## SUPPLEMENTAL DATA

Supplemental Data include four figures and can be found with this article online at http://www.immunity.com/supplemental/S1074-7613(08)00458-5.

## ACKNOWLEDGMENTS

We thank Gary Klimpel and Laurie Sower, who helped to start it all; Aynur Ekiciler, Anton Grubisic, and Thomas Stehle for expert technical assistance; and Lars Joeckel, Adrian Koch, and Praxedis Martin for providing mouse CTL lines. This work was supported in part by the grants 5RO1AI04494-03 to C.J.F and KO1 CA100095 to C.M. J.P. was supported by the Alexander von Humboldt Foundation and the Fundación Agencia Aragonesa para Investigación y Desarrollo.

Received: June 13, 2007
Revised: April 11, 2008
Accepted: August 12, 2008
Published online: October 23, 2008

## REFERENCES

Beresford, P.J., Kam, C.M., Powers, J.C., and Lieberman, J. (1997). Recombinant human granzyme A binds to two putative HLA-associated proteins and cleaves one of them. Proc. Natl. Acad. Sci. USA *94*, 9285–9290.

Beresford, P.J., Xia, Z., Greenberg, A.H., and Lieberman, J. (1999a). Granzyme A loading induces rapid cytolysis and a novel form of DNA damage independently of caspase activation. Immunity *10*, 585–594.

Beresford, P.J., Xia, Z., Greenberg, A.H., and Lieberman, J. (1999b). Granzyme A loading induces rapid cytolysis and a novel form of DNA damage independently of caspase activation. Immunity *10*, 585–594, Erratum: (1999). Immunity *10*, 768.

Beresford, P.J., Zhang, D., Oh, D.Y., Fan, Z., Greer, E.L., Russo, M.L., Jaju, M., and Lieberman, J. (2001). Granzyme A activates an endoplasmic reticulum-associated caspase-independent nuclease to induce single-stranded DNA nicks. J. Biol. Chem. *276*, 43285–43293.

Dhote, R., Simon, J., Papo, T., Detournay, B., Sailler, L., Andre, M.H., Dupond, J.L., Larroche, C., Piette, A.M., Mechenstock, D., et al. (2003). Reactive hemophagocytic syndrome in adult systemic disease: Report of twenty-six cases and literature review. Arthritis Rheum. *49*, 633–639.

Ebnet, K., Hausmann, M., Lehmann-Grube, F., Mullbacher, A., Kopf, M., Lamers, M., and Simon, M.M. (1995). Granzyme A-deficient mice retain potent cell-mediated cytotoxicity. EMBO J. *14*, 4230–4239.

Fan, Z., Beresford, P.J., Oh, D.Y., Zhang, D., and Lieberman, J. (2003a). Tumor Suppressor NM23–H1 Is a Granzyme A-Activated DNase during CTL-Mediated Apoptosis, and the Nucleosome Assembly Protein SET Is Its Inhibitor. Cell *112*, 659–672.

Fan, Z., Beresford, P.J., Zhang, D., and Lieberman, J. (2002). HMG2 interacts with the nucleosome assembly protein SET and is a target of the cytotoxic T-lymphocyte protease granzyme A. Mol. Cell. Biol. *22*, 2810–2820.

Fan, Z., Beresford, P.J., Zhang, D., Xu, Z., Novina, C.D., Yoshida, A., Pommier, Y., and Lieberman, J. (2003b). Cleaving the oxidative repair protein Ape1 enhances cell death mediated by granzyme A. Nat. Immunol. *4*, 145–153.

Franchi, L., McDonald, C., Kanneganti, T.D., Am, A., and Nunez, G. (2006). Nucleotide-binding oligomerization domain-like receptors: Intracellular pattern recognition molecules for pathogen detection and host defense. J. Immunol. *177*, 3507–3513.

Froelich, C.J., Metkar, S.S., and Raja, S.M. (2004). Granzyme B-mediated apoptosis–the elephant and the blind men? Cell Death Differ. *11*, 369–371.

Froelich, C.J., Turbov, J., and Hanna, W. (1996). Human Perforin: Rapid enrichment by immobilized metal affinity chromatography (IMAC). Biochem. Biophys. Res. Commun. *229*, 44–49.

Fruth, U., Sinigaglia, F., Schlesier, M., Kilgus, J., Kramer, M.D., and Simon, M.M. (1987). A novel serine proteinase (HuTSP) isolated from a cloned human CD8+ cytolytic T cell line is expressed and secreted by activated CD4+ and CD8+ lymphocytes. Eur. J. Immunol. *17*, 1625–1633.

Goldberg, J.E., Sherwood, S.W., and Clayberger, C. (1999). A novel method for measuring CTL and NK cell-mediated cytotoxicity using annexin V and two-color flow cytometry. J. Immunol. Methods *224*, 1–9.

Hanna, W.L., Zhang, X., Turbov, J., Winkler, U., Hudig, D., and Froelich, C.J. (1993). Rapid purification of cationic granule proteases: Application to human granzymes. Protein Expr. Purif. *4*, 398–404.

Hayes, M.P., Berrebi, G.A., and Henkart, P.A. (1989). Induction of target cell DNA release by the cytotoxic T lymphocyte granule protease granzyme A. J. Exp. Med. *170*, 933–946.

Heusel, J.W., Wesselschmidt, R.L., Shresta, S., Russell, J.H., and Ley, T.J. (1994). Cytotoxic lymphocytes require granzyme B for the rapid induction of DNA fragmentation and apoptosis in allogeneic target cells. Cell *76*, 977–987.

Hu, D., and Kipps, T.J. (1999). Reduction in mitochondrial membrane potential is an early event in Fas-independent CTL-mediated apoptosis. Cell. Immunol. *195*, 43–52.

Irmler, M., Hertig, S., MacDonald, H.R., Sadoul, R., Becherer, J.D., Proudfoot, A., Solari, R., and Tschopp, J. (1995). Granzyme A is an interleukin 1 beta-converting enzyme. J. Exp. Med. *181*, 1917–1922.

Kaiserman, D., Bird, C.H., Sun, J., Matthews, A., Ung, K., Whisstock, J.C., Thompson, P.E., Trapani, J.A., and Bird, P.I. (2006). The major human and mouse granzymes are structurally and functionally divergent. J. Cell Biol. *175*, 619–630.

Kramer, M.D., and Simon, M.M. (1987). Are proteinases functional molecules of T lymphocytes? Immunol. Today *8*, 140–143.

Maki, G., Klingemann, H.G., Martinson, J.A., and Tam, Y.K. (2001). Factors regulating the cytotoxic activity of the human natural killer cell line, NK-92. J. Hematother. Stem Cell Res. *10*, 369–383.

Martinon, F. (2007). Orchestration of pathogen recognition by inflammasome diversity: Variations on a common theme. Eur. J. Immunol. *37*, 3003–3006.

Martinvalet, D., Zhu, P., and Lieberman, J. (2005). Granzyme A induces caspase-independent mitochondrial damage, a required first step for apoptosis. Immunity *22*, 355–370.

Masson, D., and Tschopp, J. (1987). A family of serine esterases in lytic granules of cytolytic T lymphocytes. Cell *49*, 679–685.

Menasche, G., Feldmann, J., Fischer, A., and de Saint Basile, G. (2005). Primary hemophagocytic syndromes point to a direct link between lymphocyte cytotoxicity and homeostasis. Immunol. Rev. *203*, 165–179.

Metkar, S.S., Wang, B., Ebbs, M.L., Kim, J.H., Lee, Y.J., Raja, S.M., and Froelich, C.J. (2003). Granzyme B activates procaspase-3 which signals a mitochondrial amplification loop for maximal apoptosis. J. Cell Biol. *160*, 875–885.

Motyka, B., Korbutt, G., Pinkoski, M.J., Heibein, J.A., Caputo, A., Hobman, M., Barry, M., Shostak, I., Sawchuk, T., Holmes, C.F.B., et al. (2000). Mannose 6-phosphate/insulin-like growth factor II receptor is a death receptor for granzyme B during cytotoxic T cell-induced apoptosis. Cell *103*, 491–500.

Mullbacher, A., Ebnet, K., Blanden, R.V., Hla, R.T., Stehle, T., Museteanu, C., and Simon, M.M. (1996). Granzyme A is critical for recovery of mice from infection with the natural cytopathic viral pathogen, ectromelia. Proc. Natl. Acad. Sci. USA *93*, 5783–5787.

Nagahara, H., Vocero-Akbani, A.M., Snyder, E.L., Ho, A., Latham, D.G., Lissy, N.A., Becker-Hapak, M., Ezhevsky, S.A., and Dowdy, S.F. (1998). Transduction of full-length TAT fusion proteins into mammalian cells: TAT-p27Kip1 induces cell migration. Nat. Med. *4*, 1449–1452.

Pardo, J., Balkow, S., Anel, A., and Simon, M.M. (2002). The differential contribution of granzyme A and granzyme B in cytotoxic T lymphocyte-mediated apoptosis is determined by the quality of target cells. Eur. J. Immunol. *32*, 1980–1985.

Pardo, J., Bosque, A., Brehm, R., Wallich, R., Naval, J., Mullbacher, A., Anel, A., and Simon, M.M. (2004). Apoptotic pathways are selectively activated by granzyme A and/or granzyme B in CTL-mediated target cell lysis. J. Cell Biol. *167*, 457–468.

Pardo, J., Wallich, R., Martin, P., Urban, C., Rongvaux, A., Flavell, R.A., Mullbacher, A., Borner, C., and Simon, M.M. (2008). Granzyme B-induced cell

death exerted by ex vivo CTL: Discriminating requirements for cell death and some of its signs. Cell Death Differ. *15*, 567–579.

Raja, S.M., Metkar, S.S., Honing, S., Wang, B., Russin, W.A., Pipalia, N.H., Menaa, C., Belting, M., Cao, X., Dressel, R., and Froelich, C.J. (2005). A novel mechanism for protein delivery: Granzyme B undergoes electrostatic exchange from serglycin to target cells. J. Biol. Chem. *280*, 20752–20761.

Shi, L., Kraut, R.P., Aebersold, R., and Greenberg, A.H. (1992). A natural killer cell granule protein that induces DNA fragmentation and apoptosis. J. Exp. Med. *175*, 553–566.

Shiver, J.W., Su, L., and Henkart, P.A. (1992). Cytotoxicity with target DNA breakdown by rat basophilic leukemia cells expressing both cytolysin and granzyme A. Cell *71*, 315–322.

Simon, M.M., Ebnet, K., and Kramer, M.D. (1993). Molecular analysis and possible pleiotropic function(s) of the T cell-specific serine proteinase 1. In Cytotoxix Cells: Recognition, Effector Function, Generation, and Methods, M.V. Sitkovsky and P.A. Henkart, eds. (Boston: Birkhäuser), pp. 278–294.

Simon, M.M., Hoschutzky, H., Fruth, U., Simon, H.G., and Kramer, M.D. (1986). Purification and characterization of a T cell specific serine proteinase (TSP-1) from cloned cytolytic T lymphocytes. EMBO J. *5*, 3267–3274.

Sower, L.E., Froelich, C.J., Allegretto, N., Rose, P.M., Hanna, W.D., and Klimpel, G.R. (1996a). Extracellular activities of human granzyme A. Monocyte activation by granzyme A versus alpha-thrombin. J. Immunol. *156*, 2585–2590.

Sower, L.E., Klimpel, G.R., Hanna, W., and Froelich, C.J. (1996b). Extracellular activities of human granzymes. I. Granzyme A induces IL6 and IL8 production in fibroblast and epithelial cell lines. Cell. Immunol. *171*, 159–163.

van Dommelen, S.L., Sumaria, N., Schreiber, R.D., Scalzo, A.A., Smyth, M.J., and Degli-Esposti, M.A. (2006). Perforin and granzymes have distinct roles in defensive immunity and immunopathology. Immunity *25*, 835–848.

Zhang, D., Pasternack, M.S., Beresford, P.J., Wagner, L., Greenberg, A.H., and Lieberman, J. (2001). Induction of rapid histone degradation by the cytotoxic T lymphocyte protease Granzyme A. J. Biol. Chem. *276*, 3683–3690.

Zhang, D., Shankar, P., Xu, Z., Harnisch, B., Chen, G., Lange, C., Lee, S.J., Valdez, H., Lederman, M.M., and Lieberman, J. (2003). Most antiviral CD8 T cells during chronic viral infection do not express high levels of perforin and are not directly cytotoxic. Blood *101*, 226–235.